iScience

Article

Lysophosphatidylcholine induced by fat transplantation regulates hyperalgesia by affecting the dysfunction of ACC perineuronal nets

Graphical abstract

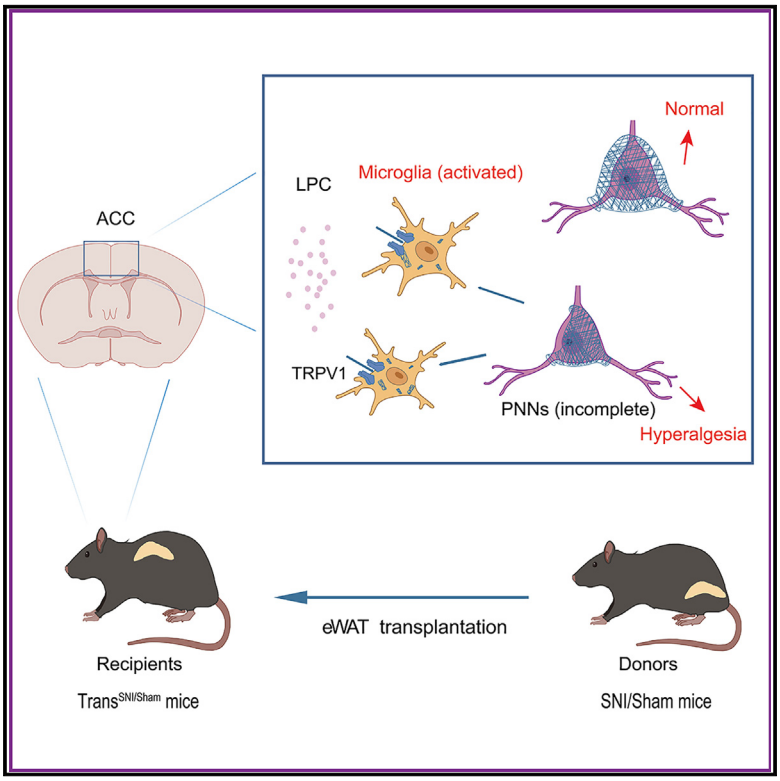

Highlights

- Adipose tissue-derived LPC plays an important role in hyperalgesia
- LPC activated ACC microglia through the TRPV1/CamkII pathway inducing hyperalgesia
- The disruption of PNNs around PV^{+} neurons in ACC promoted hyperalgesia

Authors

Juan Li, Zhen Li, Yanbo Liu, ..., Anne Manyande, Zhixiao Li, Hongbing Xiang

Correspondence

smailxiao@qq.com (Z.L.), hbxiang@tjh.tjmu.edu.cn (H.X.)

In brief

Biological sciences; Neuroscience; Cellular neuroscience

Li et al., 2024, iScience *27*, 111274
December 20, 2024 © 2024 The Authors. Published by Elsevier Inc.
https://doi.org/10.1016/j.isci.2024.111274

CellPress

iScience

CellPress
OPEN ACCESS

Article

Lysophosphatidylcholine induced by fat transplantation regulates hyperalgesia by affecting the dysfunction of ACC perineuronal nets

Juan Li,[1] Zhen Li,[1] Yanbo Liu,[1] Yijing Li,[1] Yanqiong Wu,[1] Anne Manyande,[2] Zhixiao Li,[1,*] and Hongbing Xiang[1,3,4,*]

[1]Department of Anesthesiology and Pain Medicine, Hubei Key Laboratory of Geriatric Anesthesia and Perioperative Brain Health, Wuhan Clinical Research Center for Geriatric Anesthesia, Tongji Hospital, Tongji Medical College, Huazhong University of Science and Technology, Wuhan 430030, China

[2]School of Human and Social Sciences, University of West London, London, UK

[3]Key Laboratory of Anesthesiology and Resuscitation (Huazhong University of Science and Technology), Ministry of Education, Wuhan 430030, China

[4]Lead contact

*Correspondence: smailxiao@qq.com (Z.L.), hbxiang@tjh.tjmu.edu.cn (H.X.)

https://doi.org/10.1016/j.isci.2024.111274

SUMMARY

The pathogenesis of hyperalgesia is complex and can lead to poor clinical treatment. Our study revealed that epididymal white adipose tissue (eWAT) from spared nerve injury (SNI) mice is involved in the occurrence of hyperalgesia after adipose tissue transplantation. We also showed that lysophosphatidylcholine (LPC) is enriched in the eWAT of SNI mice using non-targeted metabolomic analysis and verified that the levels of LPC in plasma and the anterior cingulate cortex (ACC) region increased following eWAT transplantation. Based on the immunohistochemistry results, we observed that LPC in the ACC region activated microglia via the TRPV1/CamkII pathway. Meanwhile, the disruption of perineuronal nets (PNNs) around PV^+ neurons in ACC promoted hyperalgesia, and the loss of PNNs and PV^+ interneurons might be due to microglial phagocytosis. These findings elucidate the mechanism underlying hyperalgesia from the perspective of lipid metabolite LPC and PNNs and provide potential strategies for the treatment of hyperalgesia.

INTRODUCTION

Adipose tissue, known to be the largest endocrine organ, can produce a broad range of bioactive factors that play an important role in communication between peripheral organs and the central nervous system.[1] Clinical studies have shown that visceral white adipose tissue is closely related to insulin resistance, hypertension, and lipid metabolism disorders.[2] A study reported that the incidence of neuropathic pain arising from non-mechanical load (such as gravity) was higher in patients with a high-BMI, while paroxysmal pain was more severe.[3] Adipose tissue secretes a variety of factors, such as IL-10, IL-6, and leptin to increase joint pain susceptibility,[4] suggesting that it has a potential role in neuropathic pain. In addition to the well-known lipid factors mentioned previously, adipose tissue can also play a role in inter-organ communication through some lipid metabolites, thus, regulating the function of recipient organs. For example, the circulating levels of visceral adipose tissue-derived serine protease inhibitor (Vaspin) could appear as a marker of musculoskeletal pain disability.[5] However, the potential role of adipose tissue-derived metabolites in neuropathic pain remains unclear.

Perineuronal nets (PNNs) are the most prominent extracellular matrix structures in the CNS. In the neocortex, PNNs particularly enwrap neuronal soma and proximal dendrites of fast-spiking parvalbumin-positive (PV^+) inhibitory interneurons, and regulate their intrinsic excitability and synaptic inputs.[6] In a recent study, the activation of microglia in the spinal cord was shown to degrade the PNNs around the projection neurons, enhance the activity of projection neurons and induce pain hypersensitivity.[7] Yet, little is known about the functional and structural changes of PNNs in brain regions associated with the hyperalgesia response. Whether adipose tissue-derived metabolites can affect changes in PNNs due to hyperalgesia remains undetermined. We investigated whether PNNs are present and affect the activity of neurons involved in the processing of nociceptive information.

In this study, we assessed the potential role of visceral adipose tissue in hyperalgesia. We conducted a non-targeted metabolomics analysis on transplanted adipose tissue to examine whether lipid-derived lysophosphatidylcholine (LPC) is a differential metabolite associated with hyperalgesia. In addition, we applied molecular biology techniques to identify the mechanism by which LPC activated microglia in the anterior cingulate cortex (ACC) of hyperalgesia mice in a recipient group to regulate the function of the perineuronal nets. The study clarified the expression level and corresponding signaling pathway changes of LPC in the ACC of the adipose tissue transplantation recipient mice. This work aimed to clarify the mechanism of hyperalgesia from

This is an open access article under the CC BY-NC-ND license (http://creativecommons.org/licenses/by-nc-nd/4.0/).

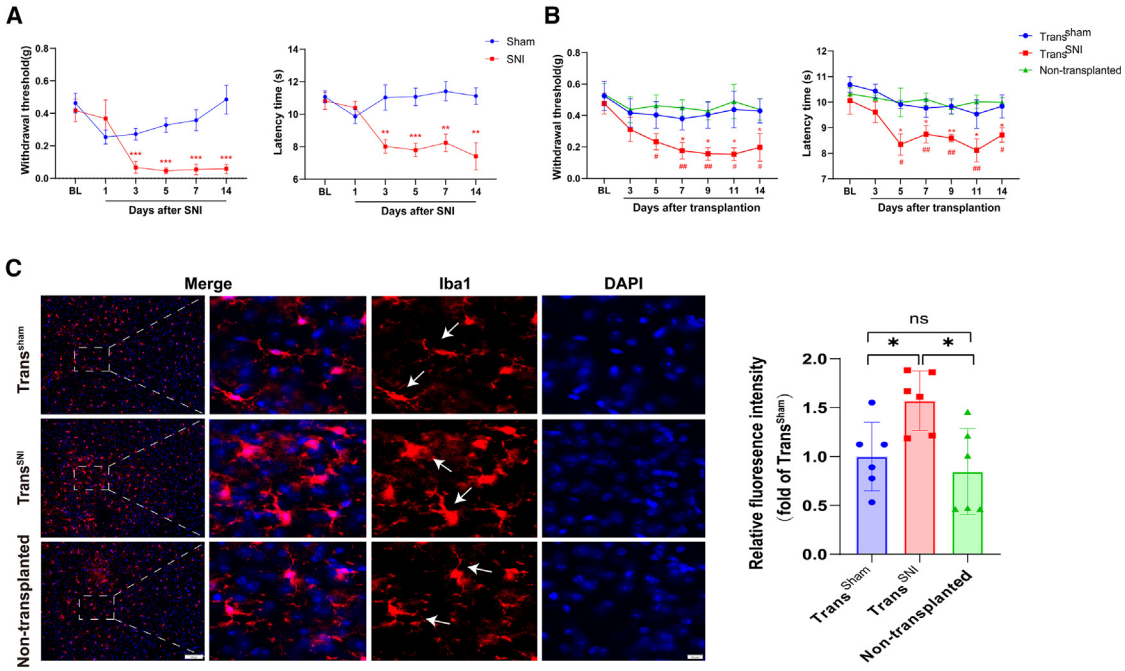

Figure 1. The pain threshold of mice changed after fat transplantation, microglia in ACC region was activated

(A) The mechanical withdrawal threshold and thermal withdrawal latency of the SNI/Sham mice, $n = 8$, SNI vs. Sham $^{*}p < 0.05$,$^{**}p < 0.01$, $^{***}p < 0.001$.

(B) The mechanical withdrawal threshold and thermal withdrawal latency of the Trans$^{SNI/Sham}$ and non-transplanted mice, $n = 8$, Trans^{SNI} vs. Trans^{sham} $^{*}p < 0.05$, $^{**}p < 0.01$; Trans^{SNI} vs. Non-transplanted $^{\#}p < 0.05$, $^{\#\#}p < 0.01$.

(C) Representative immunofluorescence staining images of microglia of the recipient and non-transplanted mice and microglia density, scale bar, 100 μm, scale bar, 10 μm, $n = 6$. Data are represented as mean ± SEM.

the perspective of lipid metabolite LPC and PNNs and to provide potential treatment strategies for hyperalgesia.

RESULTS

The fat-transplanted mice developed hyperalgesia

To determine whether adipose tissue played a role in chronic hyperalgesia of neuropathic pain, the epididymal white adipose tissue (eWAT) from spared nerve injury (SNI) mice (Trans^{SNI}) or sham mice (Trans^{Sham}) was implanted subcutaneously on the dorsum of normal mice. The SNI mouse model evoked mechanical and thermal hypersensitivity (Figure 1A). After transplantation, we observed the mechanical withdrawal threshold (MWT) and thermal withdrawal latency (TWL) of the Trans^{SNI} mice, Trans^{Sham} mice, and non-transplanted mice on the postoperative day 3, 5, 7, 9, 11, and 14. The Trans^{SNI} group of mice showed lower threshold values compared to the other two groups in MWT and TWL during day 5–14 after transplantation (Figure 1B).The immunostaining of ACC sections showed that the morphology of microglia changed and had larger cell bodies and shorter branches, and the total number of microglia cells was increased (Figure 1C).

LPC was enriched in the eWAT from SNI mice

Lipid metabolites are important modulators of adipose tissue on host pathophysiology. In order to explore the underlying mechanism of adipose tissue, we sought to detail the compositional differences between the SNI and the sham group and identify the potential deleterious product generated from adipose tissue. Thus, we performed non-targeted metabolomics analysis for adipose tissue from the two groups. The score plots of Orthogonal partial least squares-discriminant analysis (OPLS-DA) obtained from Liquid Chromatograph-Mass Spectrometer (LC-MS) data demonstrated that the metabolites of the SNI and sham group could be clearly differentiated with statistical significance (Figure 2A). The R2Ycum (0.994) and Q2cum (0.851) values exceeded 0.5, indicating that this OPLS-DA model fitted the data very well and had good predictive ability. In the permutation test, all permuted R2s and Q2s were lower than the original values on the right, suggesting that the OPLS-DA model was not random or overfitted (Figure 2A). Figure 2B illustrates the main different metabolites detected in the adipose tissue between the SNI and sham group. We focused on lysophosphatidylcholine (LPC) because it is a lysolecithin, which has been extensively linked to the generation and maintenance of pain. It was enriched in the visceral adipose tissue of mice which underwent SNI surgery. LPC is mainly derived from the turnover of phosphatidylcholine (PC) in the circulation by phospholipase A2 (PLA 2) (Figure S1).

LPC induced by eWAT in SNI mice played a crucial role in hyperalgesia

To evaluate whether LPC plays a role in hyperalgesia, we used the highly potent and selective PLA2 inhibitor varespladib to block PLA2 activity *in vivo*. Trans^{SNI} mice were administered varespladib (10 mg/kg per day for 4 days) and the LPC levels in their

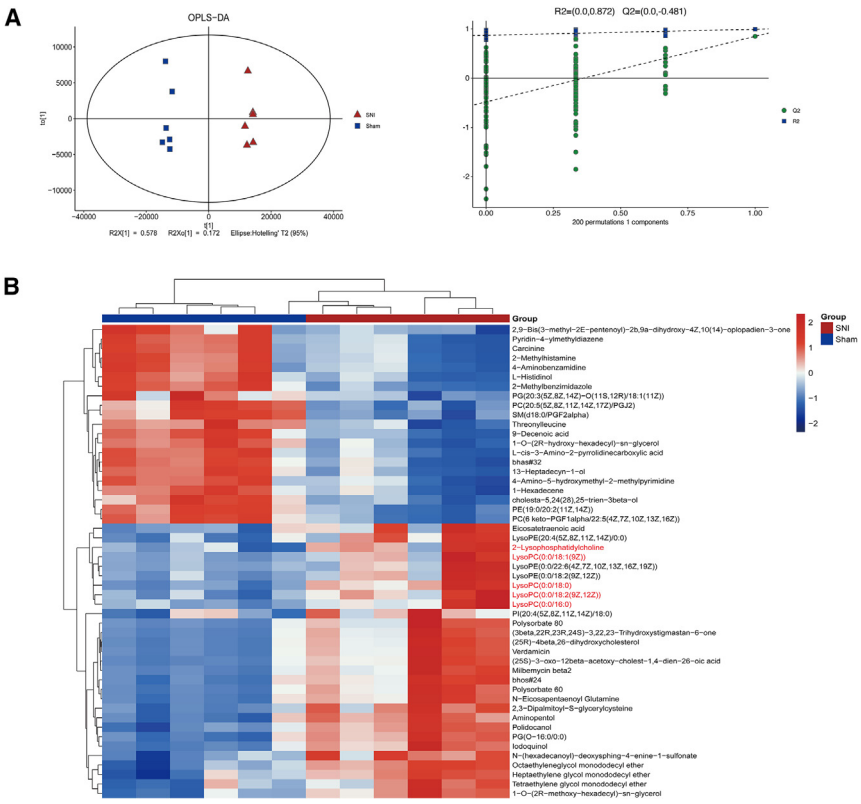

Figure 2. Non-targeted metabolomics analysis

(A) OPLS-DA.

(B) Heatmap of the hierarchical clustering analysis of differentially expressed metabolites in the top 50 VIP values, $n = 6$.

ACC region and plasma evaluated. The LPC levels in the ACC region and plasma of Trans^{SNI} mice were higher than those of Trans^{Sham} mice, and the varespladib treatment significantly diminished the LPC levels in the ACC region and plasma (Figure 3A). The varespladib remarkably relieved the mechanical and thermal hypersensitivity and inhibited microglia activation (Figures 3B and 3C). Hence, LPC is a critical regulator of hyperalgesia and microglia activation after transplantation.

LPC activated ACC microglia via the TRPV1/CamkIIpathway inducing hyperalgesia

LPC 18:1 is recognized as a previously unknown endogenous activator of the ligand-gated calcium channels transient receptor potential V1 (TRPV1) in primary sensory neurons.[8] Besides, microglial cells have an important role in initiating and maintaining pain and inflammation. Therefore, we explored the involvement of LPC in microglia activation. We compared the expression of TRPV1/p-CamkIIin the ACC between Trans^{SNI} and Trans^{Sham} groups and observed that Trans^{SNI} significantly increased the level of TRPV1 and CamkIIphosphorylationon at day 14 after transplantation (Figure 4A). TRPV1 is a non-selective ion channel that regulates the influx of Ca^{2+}, we, thus, monitored the activation of CamkII by comparing it with CamkIIphosphorylation.

In order to investigate the effect of LPC on TRPV1 activation, we tested the expression of TRPV1/p-CamkIIin the ACC after the application of varespladib. The varespladib significantly decreased the expression of TRPV1/p-CamkII (Figure 4B). The results indicate that LPC is an endogenous activator of TRPV1/CamkII. Then, we used the TRPV1 inhibitor A784168, which considerably relieved the mechanical and thermal hypersensitivity (Figure 4C). As shown in Figure 4D, the TRPV1 inhibitor A784168 notably inhibited the expression of TRPV1 and CamkII activation. Meanwhile, A784168 inhibited the activation of microglia and decreased the total number of microglia cells (Figure 4E). We performed double-labeling immunofluorescence to verify the TRPV1 channels on microglia. The Iba1-labeled microglia was closely surrounded by TRPV1 signals, that overlapped with it (Figure 4F), suggesting that LPC activated the TRPV1 channels on microglia. Next, we administered the CamkIIinhibitor KN-93, which substantially reduced the level of CamkIIphosphorylationon at day 14 (Figure 5A). It also relieved the mechanical and thermal hypersensitivity from day 11 to day 14 after transplantation and inhibited microglia activation (Figures 5B and 5C). These results imply that LPC activated microglia to regulate hyperalgesia via the TRPV1/CamkII pathway.

The degradation of the PNNs in the ACC of Trans^{SNI} mice might be due to microglial phagocytosis

The PNNs are widespread in the ACC region, which play an important role in both acute and chronic pain. Wisteria floribunda agglutinin (WFA) identified the PNNs by selectively binding the glycosaminoglycan (GAG) sugar side chains of PNN glycoproteins. We observed the degradation of PNNs in the Trans^{SNI} group as there was a significant reduction in WFA signal (Figure 6A). We administered protease-free chABC to degrade the PNNs in the ACC to verify the role of it. The MWT and TWL at 3, 7, and 14 days were significantly decreased in mice injected with chABC, and chABC caused the disappearance of PNNs in the ACC. These results indicated that PNNs played an important role in the hyperalgesia induced by transplantation (Figures 6B–6F). Recent studies revealed that microglia-mediated alterations of PNNs contribute to the pathogenesis of neurodegenerative diseases.[9,10] To study whether the degradation of the PNNs in the ACC region after transplantation is associated with microglia, we performed double labeling of Iba1 and WFA proteins. As demonstrated in Figure 7A, we observed that the total number of microglial cells increased, and the signal of PNNs declined in the Trans^{SNI} group. In addition, double immunofluorescent staining revealed co-localization of Iba1 and WFA in the Trans^{SNI} group. Then we used confocal microscope for a much clearer image. We found that the activated microglia tended to

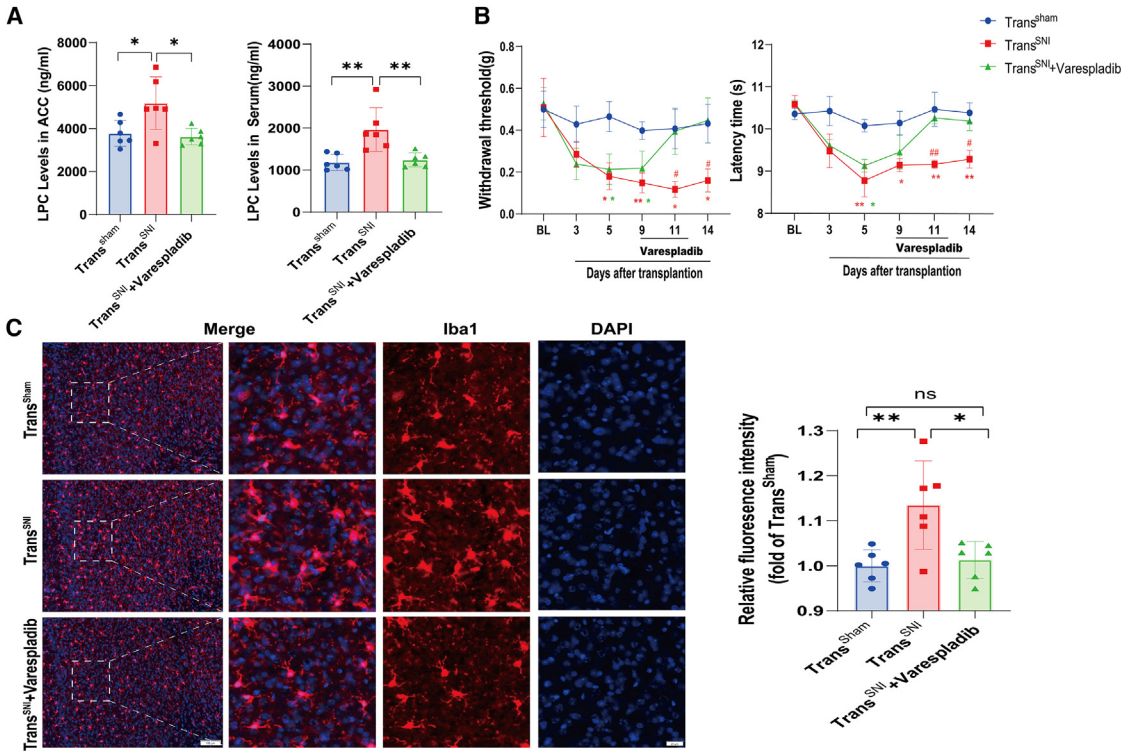

Figure 3. The varespladib relieved mechanical and thermal hypersensitivity, and inhibited microglia activation

(A) The LPC levels of the ACC region and plasma, $n = 6$, $^{*}p < 0.05$, $^{**}p < 0.01$.

(B) The mechanical withdrawal threshold and thermal withdrawal latency of the recipient mice, $n = 8$, Trans^{SNI} (Red)/Trans^{SNI} + varespladib (Green) vs. Trans^{sham} $^{*}p < 0.05$, $^{**}p < 0.01$; Trans^{SNI} vs. Trans^{SNI} + varespladib $^{\#}p < 0.05$, $^{\#\#}p < 0.01$.

(C) Representative immunofluorescence staining images of microglia of the recipient mice and microglia density, scale bar, 100 μm, scale bar, 20 μm, $^{*}p < 0.05$, $^{**}p < 0.01$, $n = 6$. Data are represented as mean ± SEM.

actively move around the PNNs in one fluorescence section, and numerous microglia contained WFA immunoreactivity within their body in another fluorescence section in the Trans^{SNI} group (Figure 7B), indicating that microglial cells might be phagocytosing PNNs. This phenomenon existed only in the Trans^{SNI} group. No WFA signal was detected within microglial body of the control group.

Inhibitory interneurons had abnormal discharge in Trans^{SNI} mice

Given that inhibitory interneurons in the ACC region are essential in controlling pain, we recorded the firing rates of inhibitory interneurons in the ACC region with a patch-clamp (Figure 8A). We found a significant reduction in the amplitude of miniature inhibitory postsynaptic currents (mIPSCs) in the Trans^{SNI} mice group. Although there was no difference in the frequency of mIPSCs between the two groups (Figure 8B), we observed abnormal firing properties of inhibitory interneurons in Trans^{SNI} mice. PNNs primarily wrap around certain neurons in the central nervous system and have a widely known role of protective barrier. The abundance of PNNs in the ACC region was reduced, leading to the exposure of inhibitory interneurons and thus their dysfunction. Hyperalgesia was the negative consequence resulting from the exposure.

Disruption of PNNs around PV^{+} neurons in ACC promoted hyperalgesia

In the ACC, PNNs particularly enwrap neuronal soma and proximal dendrites of fast-spiking PV^{+} inhibitory interneurons, which can regulate their intrinsic excitability and synaptic inputs. Therefore, we performed double labeling of PV^{+} and WFA proteins. PNNs mainly enwrapped parvalbumin-positive inhibitory interneurons in the ACC of the two groups. The number of PV^{+} neurons and the fluorescence intensity of PNNs significantly decreased in the Trans^{SNI} group (Figure 9A). Microglia are currently considered to be unique phagocytes in the brain. In the state of hyperalgesia, we explored the relationship between microglia and PV^{+} neurons. The immunostaining sections of Trans^{SNI} mice showed that the morphology of microglia changed, and the total number of microglia cells was increased. We also observed that the number of PV^{+} neurons in the Trans^{SNI} group reduced, while, some microglia enwrapped the PV^{+} neurons. From a much clearer image made using a confocal microscope, we found branches of a microglia enwrapping PV^{+} neurons (Figure 9B). But this phenomenon did not exist in the Trans^{Sham} group. Additionally, as demonstrated in Figure S2, we observed that chABC caused the disappearance of PNNs around PV^{+} neurons in the ACC, and there was no difference in the number of PV^{+} neurons between the chABC and control

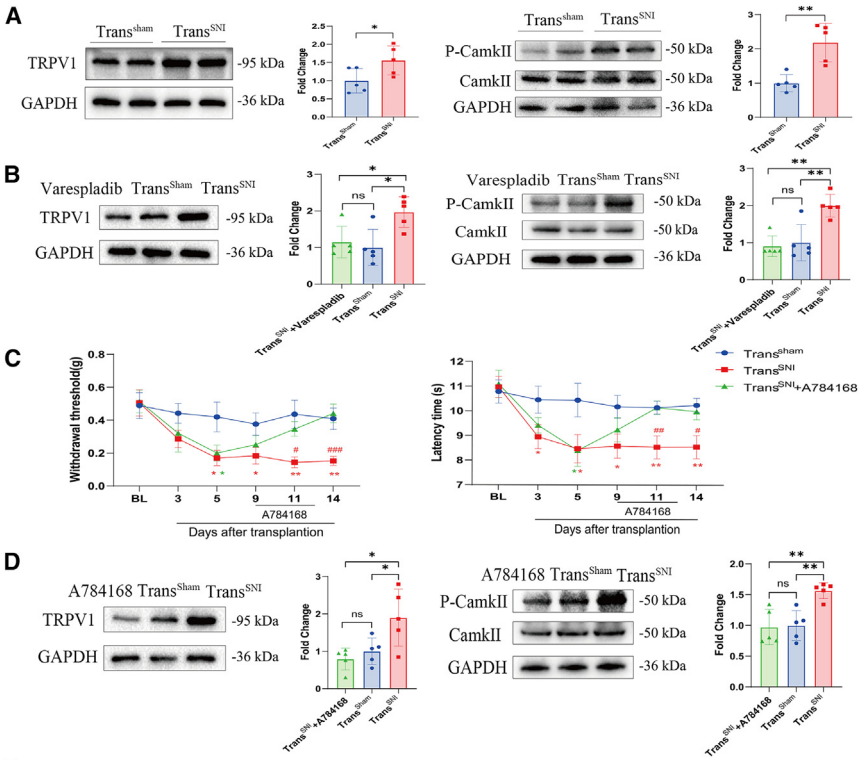

Figure 4. LPC activated microglia regulating hyperalgesia via the TRPV1/CamkII pathway

(A) The TRPV1/p-CamkII levels of the ACC region in Trans^{SNI} and Trans^{sham} mices, $^{*}p < 0.05$, $^{**}p < 0.01$, $n = 5$.

(B) The TRPV1/p-CamkII levels of the ACC region in the Trans^{SNI}, Trans^{sham}, and Trans^{SNI} + varespladib mice, $^{*}p < 0.05$, $^{**}p < 0.01$, $n = 5$.

(C) The mechanical withdrawal threshold and thermal withdrawal latency of the recipient mice, $n = 8$, Trans^{SNI} (Red)/Trans^{SNI} +A784168 (Green) vs. Trans^{sham}, $^{*}p < 0.05$, $^{**}p < 0.01$; Trans^{SNI} vs. Trans^{SNI} +A784168, $^{\#}p < 0.05$, $^{\#\#}p < 0.01$, $^{\#\#\#}p < 0.001$.

(D) The TRPV1/p-CamkII levels of the ACC region in the Trans^{SNI}, Trans^{sham}, and Trans^{SNI} + A784168 mice, $^{*}p < 0.05$, $^{**}p < 0.01$, $n = 5$.

(E) Representative immunofluorescence staining images of microglia of the recipient mice and microglia density, $^{*}p < 0.05$, scale bar, 100 μm, scale bar, 20 μm, $n = 6$.

(F) Representative immunofluorescence staining images of double labeling TRPV1 and Iba1, scale bar, 20 μm, scale bar, 7.5 μm. Data are represented as mean ± SEM.

group. These collective results suggest that the loss of PNNs and PV^{+} interneurons might be due to microglial phagocytosis. The finding may shed further light on the underlying mechanism of hyperalgesia induced by fat transplantation.

DISCUSSION

In this study, we revealed the role of adipose tissue in the development of hyperalgesia. The principal findings are as follows: (1) The recipient mice that received eWAT of SNI mice developed hyperalgesia. LPC was enriched in the eWAT of SNI mice, indicating that LPC plays an important role in hyperalgesia; (2) LPC in the ACC region activated microglial cells through the TRPV1/CamkII pathway; (3) Disruption of PNNs around PV^{+} neurons in ACC promoted hyperalgesia, and the degradation of PNNs may be mediated by microglia.

Visceral white adipose tissue is involved in the occurrence of hyperalgesia

The adipose tissue in mammals can be classified into WAT which primarily stores energy and participates in endocrine functions, BAT, which mainly generates heat and energy to maintain core body temperature, and beige adipose tissue.[11] WAT is the main adipose tissue present in adolescents and adults, as the BAT mass decreases with age in humans.[12] Clinical studies have determined that visceral white adipose tissue (vWAT) is closely associated with insulin resistance, hypertension, and lipid metabolism disorders[2] and produces various bioactive factors that coordinate with the central or peripheral nervous system.[1] Research has also shown that visceral adipose tissue-derived extracellular vesicles mediate adipose tissue-brain inter-organ communication, and induce cognitive impairment associated with insulin resistance.[13] Regarding the relationship between adipose tissue and pain, a study reported that the incidence of neuropathic pain arising from non-mechanical load (such as gravity) was higher in the high-BMI patients, while paroxysmal pain was more severe.[3] Furthermore, adipose

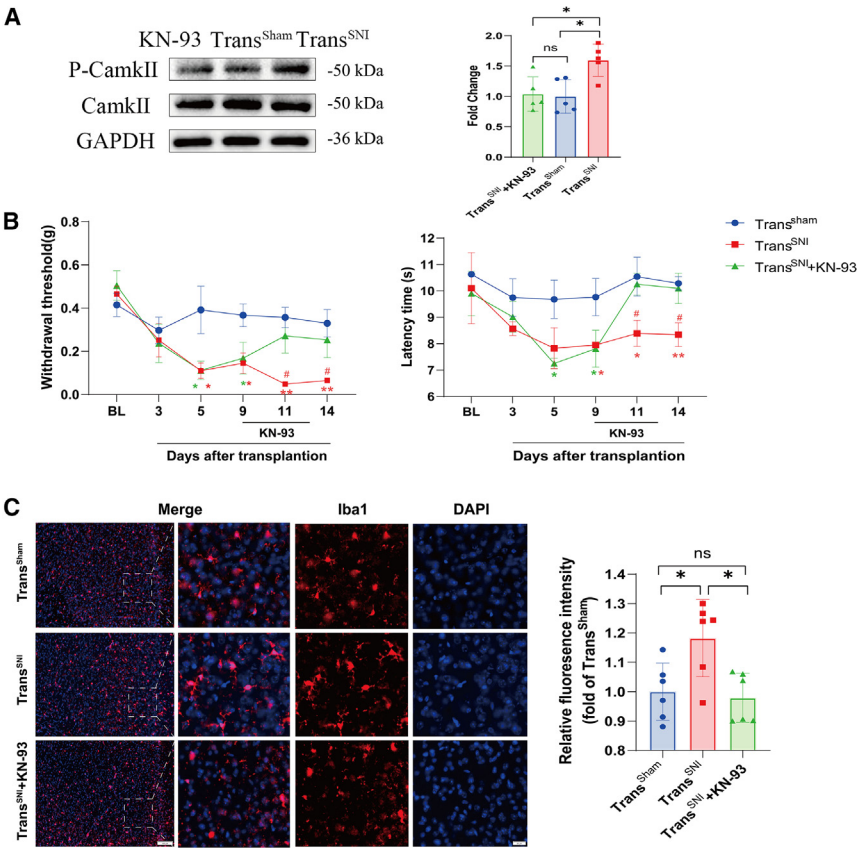

Figure 5. KN-93 reduced the level of CamkII-phosphorylationon and relieved the mechanical and thermal hypersensitivity after transplantation, and inhibited microglia activation

(A) The p-CamkII levels of the ACC region in the Trans^{SNI}, Trans^{sham}, and Trans^{SNI} +KN-93 mice, $^{*}p < 0.05$, $n = 5$.

(B) The mechanical withdrawal threshold and thermal withdrawal latency of the recipient mice, $n = 8$, Trans^{SNI} (Red)/Trans^{SNI} +KN-93 (Green) vs. Trans^{sham}, $^{*}p < 0.05$, $^{**}p < 0.01$; Trans^{SNI} vs. Trans^{SNI} +KN-93, $^{\#}p < 0.05$, $^{\#\#}p < 0.01$.

(C) Representative immunofluorescence staining images of microglia of the recipient mice and microglia density, $^{*}P < 0.05$, Scale bar = 100 μm, Scale bar, 20 μm, $n = 6$. Data are represented as mean ± SEM.

tissue alterations are known to increase neuropathic pain by activating the AMPK-ERK-NOX4 pathway.[14] These studies suggest that adipose tissue has a potential role in neuropathic pain. To validate the role of vWAT in chronic hyperalgesia of neuropathic pain, we performed adipose tissue transplantation. Our findings are consistent with previous studies. The Trans^{SNI} mice exhibited hyperalgesia from day 5 to 14 after transplantation, indicating the involvement of adipose tissue in neuropathic pain. Our immunostaining of ACC sections showed changes in the morphology of microglia cells, including enlarged cell bodies, shortened processes, and increased the total number of microglia cells.

LPC induced by fat transplantation played a crucial role in hyperalgesia

LPC is a bioactive pro-inflammatory lipid. In response to lipid peroxidation as a result of inflammation and tissue injury, phospholipids undergo lipid peroxidation to LPC.[15] Exposure to endogenous and exogenous LPC can trigger inflammatory cascades under chronic disease conditions,[16] such as diabetes, cancer, cardiovascular disease, or neurodegenerative diseases.[17,18] Oxidative stress and inflammation are underlying mechanisms of chronic pain.[19] We have established that LPC was enriched in the visceral adipose tissue of SNI-operated mice using non-targeted metabolomics analysis. Additionally, LPC levels increased in the ACC region and plasma of the Trans^{SNI} group mice. Different forms of LPC exist in various cellular and tissue systems, but the LPC in the brain mainly originates from blood, transmitted through specific LPC receptors on the blood-brain barrier.[20,21] Elevated LPC levels in plasma may occur through two possible pathways: firstly, LPC-rich adipose tissue in SNI mice may release LPC into the bloodstream via paracrine, endocrine, or autocrine pathways; secondly, LPC may act as a pro-inflammatory mediator that triggers systemic inflammation and increases LPC production throughout the body.[22,23] PLA2 is a key enzyme in the generation of LPC. Therefore, we administered the PLA2 inhibitor varespladib to block PLA2 activity and reduce LPC levels in the body. Our results showed that the varespladib treatment significantly reduced the LPC levels in the ACC region and plasma of Trans^{SNI} mice. The varespladib markedly alleviated mechanical and thermal hypersensitivity and inhibited microglia activation. Our results are in line with previous studies, illustrating that cauda equina compression (CEC) can develop into neuropathic pain while cerebrospinal fluid and plasma levels of various LPC species, especially LPC (16:0), LPC (18:2), and LPC (20:4), significantly increase in CEC model rats or patients with lumbar spinal stenosis (LSS).[24] In a clinical study of 650 patients with multisite musculoskeletal pain from Newfoundland, the level of LPC in patients was positively correlated with multisite musculoskeletal pain.[25] Numerous studies have demonstrated that levels of LPC in animal or human body fluids or tissues are elevated in various chronic pain states, including chronic inflammatory pain, chronic joint pain, neuropathic pain, and fibromyalgia. Our study revealed that LPC is a critical regulator of hyperalgesia signaling that it might be an interesting target for biomarkers and an opportunity to develop chronic pain medicine.

The level of LPC is closely related to the activation of microglia. Although it has been shown that LPC induces intracellular Ca^{2+} influx and morphological changes in microglia from ramified into ameboid microglia,[26] a study has uncovered that

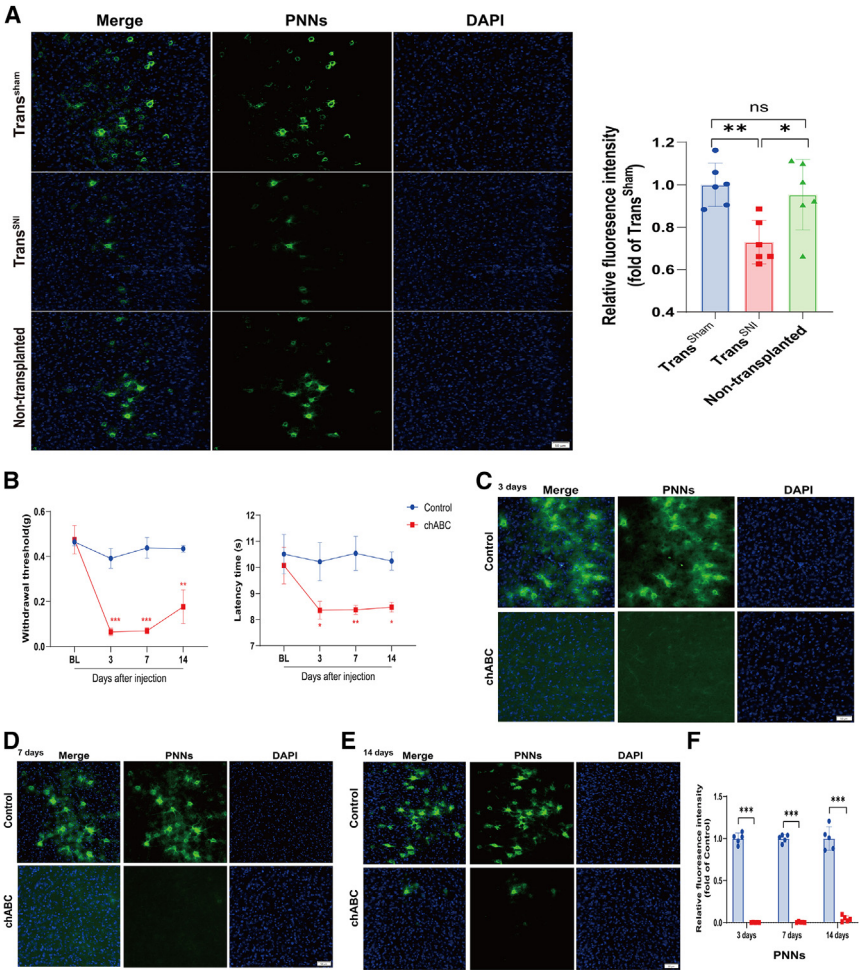

Figure 6. PNNs played an important role in the hyperalgesia induced by transplantation

(A) Representative immunofluorescence staining images of PNNs of the recipient and non-transplanted mice and PNNs density, scale bar, 50 μm, $n = 6$, $^{*}p < 0.05$, $^{**}p < 0.01$.

(B) The injection of chABC lead to the development of hyperalgesia, $n = 6$, $^{*}p < 0.05$,$^{**}p < 0.01$, $^{***}p < 0.001$.

(C–F) Images and quantification showing elimination of PNNs in chABC group on day 3,7, and 14 after injection, scale bar, 50 μm, $n = 5$ $^{*}p < 0.05$, $^{**}p < 0.01$, $^{***}p < 0.001$. Data are represented as mean ± SEM.

LPC can mediate glia activation via the Rho kinase-dependent pathway.[27] We also found that the ACC region of Trans^{SNI} mice notably elevated the level of TRPV1 and CamkIIphosphorylation after transplantation. TRPV1 is a non-selective ion channel that regulates the influx of Ca^{2+}. In a study of itch, LPC was shown to activate skin innervating TRPV1^{+} pruriceptor sensory neurons and for LPA to directly activate TRPA1 and TRPV1.[28,29] Another study reported that TRPV1 is a critical neuropathic pain biomarker, primarily functioning in microglial cells rather than neurons in the ACC region.[30] Our proteins and double labeling of Iba1 and TRPV1 results also demonstrated this point. The varespladib substantially reduced the expression of TRPV1/p-CamkII. The results indicate that LPC is an endogenous activator of the TRPV1/CamkII pathway. When, we used the TRPV1 inhibitor A784168 and the CamkII inhibitor KN-93, they significantly alleviated mechanical and thermal hypersensitivity, as well as inhibited the expression of TRPV1 and CamkII activation. Meanwhile, A784168 and KN-93 inhibited the activation of microglia and decreased the total number of microglia cells. These results suggest that LPC activated the TRPV1 channels on microglia to mediate microglia activation consequently inducing hyperalgesia.

Activated microglia promoted the degradation of PNNs in the ACC

PNNs are the most prominent extracellular matrix structures in the CNS, crucial for regulating and stabilizing neuroplasticity and synaptic activity during development and adulthood.[31] In the neocortex, PNNs particularly enwrap neuronal soma and proximal dendrites of fast-spiking parvalbumin-positive inhibitory interneurons, and regulate their intrinsic excitability and synaptic inputs.[6] A study revealed that perineuronal nets were associated rather rarely to pyramidal cells compared to inhibitory interneurons in layers II/III and V/VI of rat neocortex.[32] At the cellular level, CaMKII is mainly expressed in excitatory pyramidal neurons in the cortex. As shown in Figure S3, a large proportion of PNNs was co-localized with inhibitory PV^{+} neurons but not with CaMKII-IR neurons in the ACC. Therefore, we only focused on the PNNs around PV^{+} neurons in this study. Recent studies have shown that PNNs in various brain regions of the central nervous system can participate in the regulation of pain. Two key components of PNNs, hapln1, and aggrecan, were considerably reduced in the hippocampus of chronic pain mice.[33] In addition, it has been reported that microglia degrade PNNs which selectively enwrap spinoparabrachial projection neurons after peripheral nerve injury, thereby enhancing the activity of projection neurons and inducing pain-related behaviors.[34] Mascio et al. reported that PNNs degradation induced by intracortical infusion of chondroitinase-ABC significantly lowered mechanical and thermal pain in complete Freund's adjuvant (CFA)-injected mice.[35] These studies confirm the important role of PNNs in pain. Our study showed that PNNs in the ACC region of mice displaying hyperalgesia was extensively degraded, which is consistent with previous research. Different brain regions play different roles in pain, so the regulation of PNNs in different brain regions also varies. For example, the degradation of PNNs in the somatosensory cortex alleviates pain, but in the ACC area, it is completely reversed.

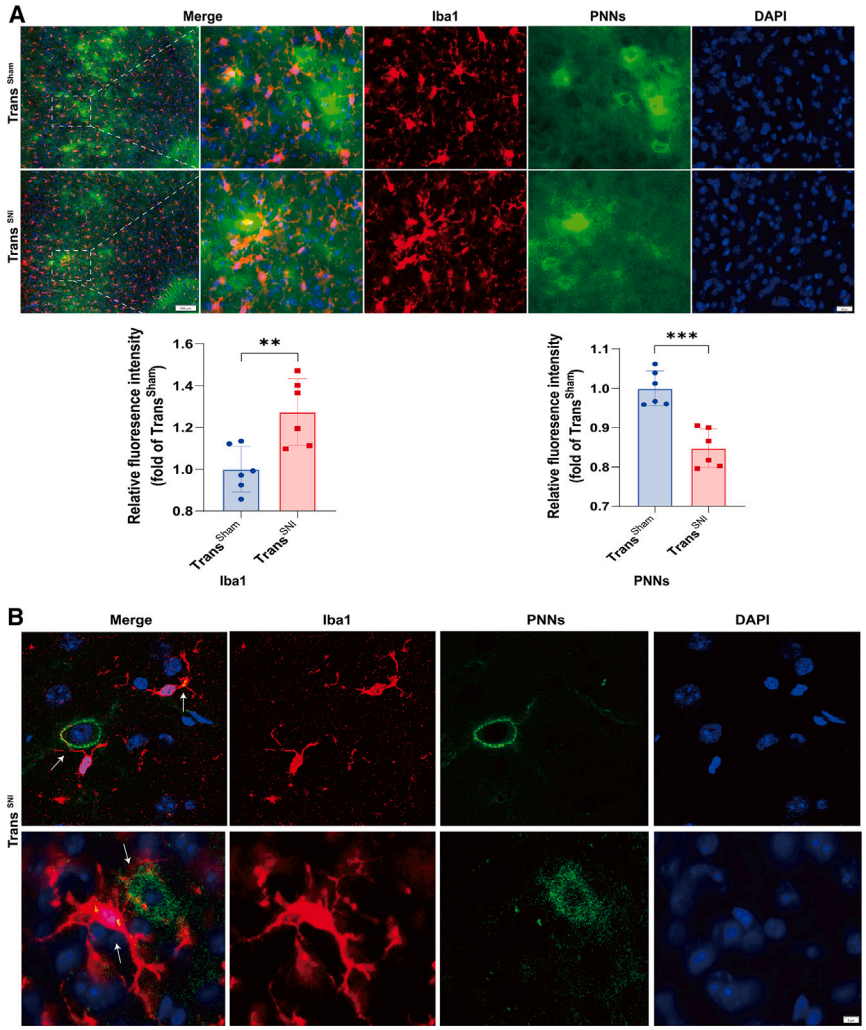

Figure 7. The degradation of the PNNs in the ACC of Trans^{SNI} mice might be due to microglial phagocytosis

(A) Represent images of double labeling PNNs and Iba1 in the recipient mice, scale bar, 100 μm, scale bar, 20 μm, $n = 6$, $^{**}p < 0.01$, $^{***}p < 0.001$.

(B) Different sections represent images of double labeling PNNs and Iba1 of the Trans^{SNI} mice, scale bar, 20 μm. Data are represented as mean ± SEM.

The loss of PV$^+$ interneurons induced hyperalgesia

Inhibitory interneurons in the ACC region are essential in controlling pain.[36,37] An earlier study conducted multiple whole-cell recordings of neurons in layer 5 (L5) of the ACC of adult mice after chronic constriction injury to the sciatic nerve of the left hind paw. They observed a decrease in mEPSC and mIPSC frequencies.[38] We recorded the firing rates of inhibitory interneurons in the ACC region with a patch-clamp. We found a noteworthy decline in the amplitude of mIPSCs in the Trans^{SNI} mice group. There was also no difference in the frequency of mIPSCs between two the groups. The result indicates that the function of postsynaptic membrane receptors of inhibitory interneurons had changed. Our results are consistent with previous findings. In the ACC, PNNs particularly enwrap PV$^+$ inhibitory interneurons, acting as protective barriers. We considered that the reduced abundance of PNNs in the ACC area exposed inhibitory interneurons, and led to their disruption. Hyperalgesia is the adverse consequence of this exposure. PV$^+$ neurons are a type of inhibitory GABAergic interneuron, widely distributed in the whole pathway for pain transmission from the peripheral nociceptive terminals to the central nervous system.[39,40] Researchers have reported that SNI increased levels of Piezo1 protein in PV$^+$ interneurons in the bilateral ACC. In addition, they observed a decrease in the number of PV$^+$ interneurons in the SNI chronic pain model. Combined with the encapsulation of Piezo1-positive neurons by Iba1 microglia, this study indicates that the loss of PV$^+$ interneurons after SNI might be due to microglial phagocytosis.[41] Our results also uncovered a significant decline in the number of PV$^+$ neurons in the Trans^{SNI} group, with microglia enwrapping the PV$^+$ neurons. We believe that the loss of PV$^+$ neurons in the Trans^{SNI} mice might be due to the phagocytic action of microglial cells, which led to changes in the function of postsynaptic membrane receptors of inhibitory interneurons and caused hyperalgesia.

Limitations of the study

In addition to the ACC region, PNNs also exist in other brain regions of the central nervous system, such as somatosensory cortex and hippocampal region. In the present study, we focused on the ACC region, which plays an important role in hyperalgesia. Further studies will be performed to examine the function of PNNs in other brain regions. Furthermore, we only studied the role of LPC and PNNs in hyperalgesia of male mice. We will elucidate the precise mechanism of LPC and PNNs in hyperalgesia of female mice in a further study and provide potential treatment strategies for hyperalgesia.

Conclusions

Our study revealed a mechanism whereby visceral adipose tissue is involved in hyperalgesia. LPC was enriched in the eWAT from SNI mice, which increased the levels of LPC in the plasma and ACC region. The LPC activated microglia via the TRPV1/CamkII pathway. The disruption of PNNs around PV$^+$ neurons in ACC promoted hyperalgesia, and the loss of PNNs and PV$^+$ interneurons might be due to microglial phagocytosis. These findings elucidate the mechanism of hyperalgesia from the perspective of lipid metabolite LPC and PNNs, and provide potential treatment strategies for hyperalgesia.

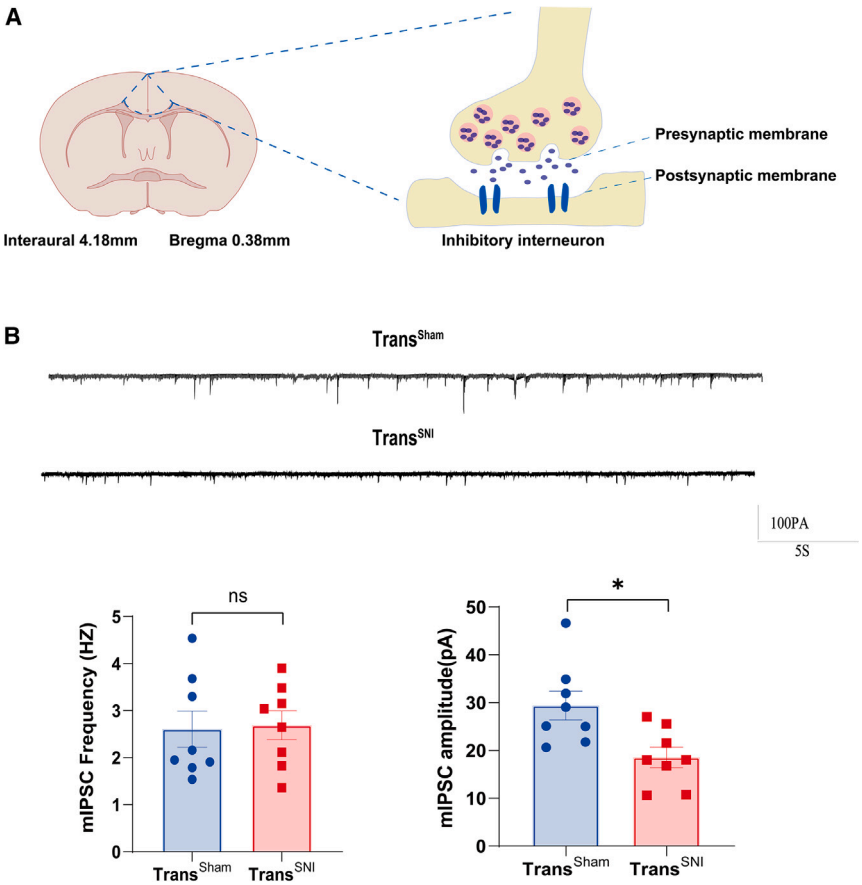

Figure 8. Inhibitory interneurons had abnormal discharge in Trans^{SNI} mice

(A) Recorded the firing rates of inhibitory interneurons in the ACC region with a patch-clamp.

(B) The amplitude and frequency of mIPSCs in Trans$^{SNI/Sham}$ mice, $^{*}p < 0.05$, $n = 8$. Data are represented as mean ± SEM.

RESOURCE AVAILABILITY

Lead contact

Further information and requests for resources and reagents should be directed to the lead contact, Hongbing Xiang (hbxiang@tjh.tjmu.edu.cn).

Materials availability

This study did not generate new unique reagents.

Data and code availability

- The datasets used and/or analyzed during the current study are available within the manuscript and its supplementary information files.
- Raw data of non-targeted metabolomic analysis is deposited and publically available at https://ngdc.cncb.ac.cn/omix: accession no. OMIX007437.
- Any additional information required in this paper is available from the lead contact upon request.

ACKNOWLEDGMENTS

This work was supported by the National Natural Science Foundation of China (No. 81873467) and Hubei Provincial Finance Project (Clinical Discipline Capability Enhancement Direction).

AUTHOR CONTRIBUTIONS

J.L., H.X., and Zhixiao L. designed the experiments and oversaw all aspects of study conduct and manuscript preparation. J.L., Zhen L., Y.Liu, and Y.Li. performed the experiments. J.L. and Y.W., analyzed the data. J.L., A.M., and H.X. wrote and edited the paper.

DECLARATION OF INTERESTS

The authors declare no competing interests.

STAR★METHODS

Detailed methods are provided in the online version of this paper and include the following:

- KEY RESOURCES TABLE
- EXPERIMENTAL MODEL AND STUDY PARTICIPANT DETAILS
  - Animals
- METHOD DETAILS
  - Spared nerve injury (SNI)
  - Epididymal white adipose tissue transplantation
  - Behavioral test
  - Non-targeted metabolomic analysis
  - Immunohistochemistry
  - Elisa test
  - Western blot analysis
  - In vivo pharmacological studies
  - ACC injection
  - Electrophysiology recording
- QUANTIFICATION AND STATISTICAL ANALYSIS

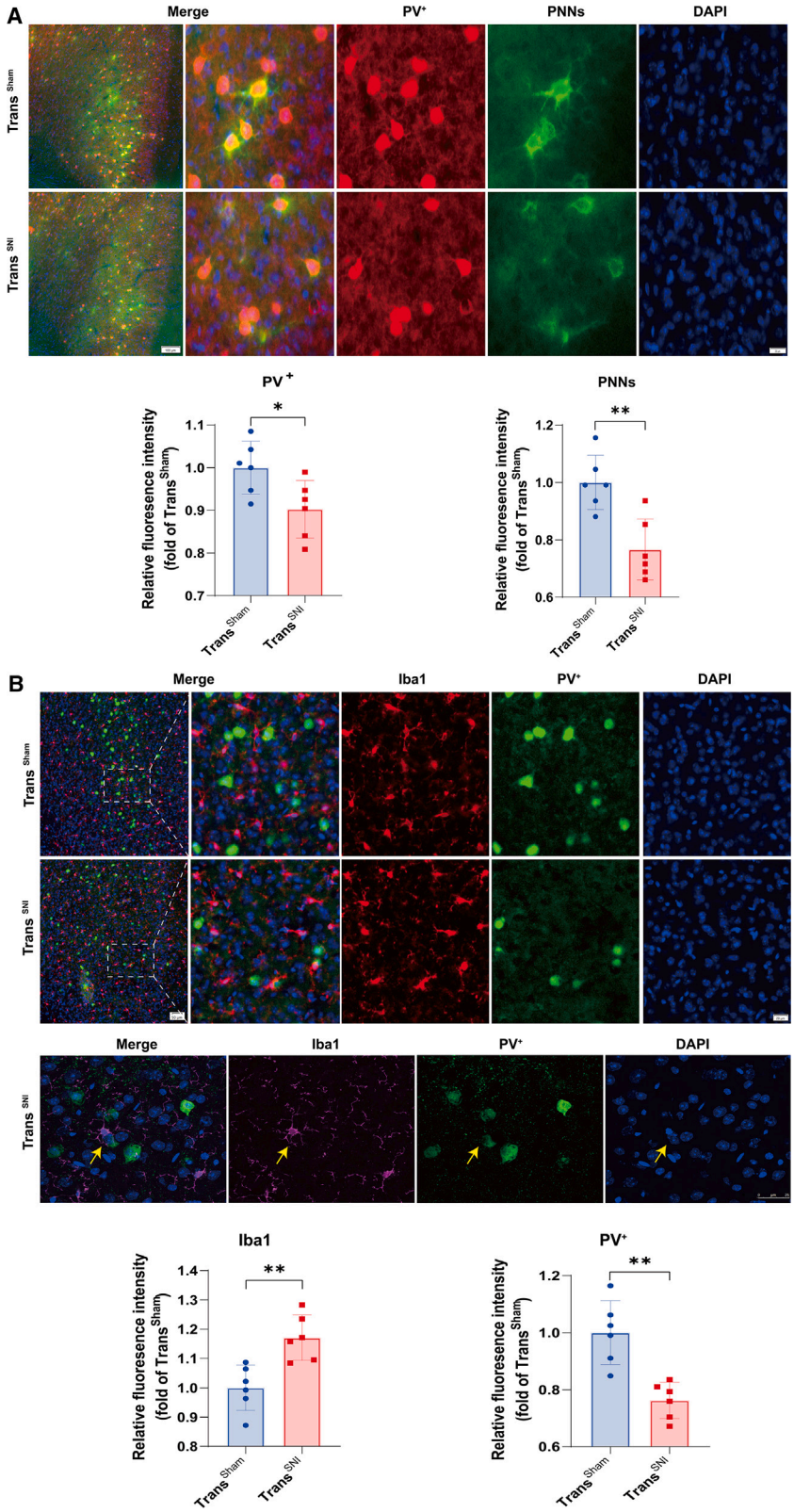

Figure 9. Disruption of PNNs around PV$^+$ neurons promoted hyperalgesia

(A) Representative images of double labeling PV$^+$ and PNNs using a virtual slide microscope in the recipient mice, $^*p < 0.05$, $^{**}p < 0.01$, scale bar, 100 μm, scale bar, 20 μm, $n = 6$.

(B) Representative images of double labeling PV$^+$ and Iba1 utilizing virtual slide microscope in the recipient mice, $^{**}p < 0.01$, scale bar, 50 μm, scale bar, 20 μm, $n = 6$. High-magnification representative images of double labeling PV$^+$ and Iba1 using confocal microscope in the Trans^{SNI} mice, scale bar, 25 μm. Data are represented as mean ± SEM.

SUPPLEMENTAL INFORMATION

Supplemental information can be found online at https://doi.org/10.1016/j.isci.2024.111274.

Received: March 4, 2024
Revised: June 12, 2024
Accepted: October 25, 2024
Published: November 5, 2024

REFERENCES

1. Greenhill, C. (2017). Adipose tissue: Crosstalk between adipocytes and neurons. Nat. Rev. Endocrinol. *13*, 438. https://doi.org/10.1038/nrendo.2017.79.
2. Tchernof, A., and Després, J.P. (2013). Pathophysiology of human visceral obesity: an update. Physiol. Rev. *93*, 359–404. https://doi.org/10.1152/physrev.00033.2011.
3. Hozumi, J., Sumitani, M., Matsubayashi, Y., Abe, H., Oshima, Y., Chikuda, H., Takeshita, K., and Yamada, Y. (2016). Relationship between Neuropathic Pain and Obesity. Pain Res. Manag. *2016*, 2487924. https://doi.org/10.1155/2016/2487924.
4. Collins, K.H., Lenz, K.L., Pollitt, E.N., Ferguson, D., Hutson, I., Springer, L.E., Oestreich, A.K., Tang, R., Choi, Y.R., Meyer, G.A., et al. (2021). Adipose tissue is a critical regulator of osteoarthritis. Proc Natl Acad Sci USA *118*, e2021096118. https://doi.org/10.1073/pnas.2021096118.
5. Tarabeih, N., Kalinkovich, A., Shalata, A., and Livshits, G. (2020). Circulating Levels of Visceral Adipose Tissue-Derived Serine Protease Inhibitor (Vaspin) Appear as a Marker of Musculoskeletal Pain Disability. Diagnostics *10*, 797. https://doi.org/10.3390/diagnostics10100797.
6. Favuzzi, E., Marques-Smith, A., Deogracias, R., Winterflood, C.M., Sánchez-Aguilera, A., Mantoan, L., Maeso, P., Fernandes, C., Ewers, H., and Rico, B. (2017). Activity-Dependent Gating of Parvalbumin Interneuron Function by the Perineuronal Net Protein Brevican. Neuron *95*, 639. https://doi.org/10.1016/j.neuron.2017.06.028.
7. Tansley, S., Gu, N., Guzmán, A.U., Cai, W., Wong, C., Lister, K.C., Muñoz-Pino, E., Yousefpour, N., Roome, R.B., Heal, J., et al. (2022). Microglia-mediated degradation of perineuronal nets promotes pain. Science *377*, 80–86. https://doi.org/10.1126/science.abl6773.
8. Rimola, V., Hahnefeld, L., Zhao, J., Jiang, C., Angioni, C., Schreiber, Y., Osthues, T., Pierre, S., Geisslinger, G., Ji, R.R., et al. (2020). Lysophospholipids Contribute to Oxaliplatin-Induced Acute Peripheral Pain. J. Neurosci. *40*, 9519–9532. https://doi.org/10.1523/jneurosci.1223-20.2020.
9. Arreola, M.A., Soni, N., Crapser, J.D., Hohsfield, L.A., Elmore, M.R.P., Matheos, D.P., Wood, M.A., Swarup, V., Mortazavi, A., and Green, K.N. (2021). Microglial dyshomeostasis drives perineuronal net and synaptic loss in a CSF1R(+/-) mouse model of ALSP, which can be rescued via CSF1R inhibitors. Sci. Adv. *7*, eabg1601. https://doi.org/10.1126/sciadv.abg1601.
10. Crapser, J.D., Ochaba, J., Soni, N., Reidling, J.C., Thompson, L.M., and Green, K.N. (2020). Microglial depletion prevents extracellular matrix changes and striatal volume reduction in a model of Huntington's disease. Brain *143*, 266–288. https://doi.org/10.1093/brain/awz363.
11. Zwick, R.K., Guerrero-Juarez, C.F., Horsley, V., and Plikus, M.V. (2018). Anatomical, Physiological, and Functional Diversity of Adipose Tissue. Cell Metabol. *27*, 68–83. https://doi.org/10.1016/j.cmet.2017.12.002.
12. Pfannenberg, C., Werner, M.K., Ripkens, S., Stef, I., Deckert, A., Schmadl, M., Reimold, M., Häring, H.U., Claussen, C.D., and Stefan, N. (2010). Impact of age on the relationships of brown adipose tissue with sex and adiposity in humans. Diabetes *59*, 1789–1793. https://doi.org/10.2337/db10-0004.
13. Wang, J., Li, L., Zhang, Z., Zhang, X., Zhu, Y., Zhang, C., and Bi, Y. (2022). Extracellular vesicles mediate the communication of adipose tissue with brain and promote cognitive impairment associated with insulin resistance. Cell Metabol. *34*, 1264. https://doi.org/10.1016/j.cmet.2022.08.004.
14. Fu, C.N., Wei, H., Gao, W.S., Song, S.S., Yue, S.W., and Qu, Y.J. (2021). Obesity increases neuropathic pain via the AMPK-ERK-NOX4 pathway in rats. Aging (Albany NY) *13*, 18606–18619. https://doi.org/10.18632/aging.203305.
15. Qin, Z.X., Zhu, H.Y., and Hu, Y.H. (2009). Effects of lysophosphatidylcholine on beta-amyloid-induced neuronal apoptosis. Acta Pharmacol. Sin. *30*, 388–395. https://doi.org/10.1038/aps.2009.25.
16. Ren, J., Lin, J., Yu, L., and Yan, M. (2022). Lysophosphatidylcholine: Potential Target for the Treatment of Chronic Pain. Int. J. Mol. Sci. *23*, 8274.
17. Nikolaou, A., Kokotou, M.G., Vasilakaki, S., and Kokotos, G. (2019). Small-molecule inhibitors as potential therapeutics and as tools to understand the role of phospholipases A(2). Biochim. Biophys. Acta Mol. Cell Biol. Lipids *1864*, 941–956. https://doi.org/10.1016/j.bbalip.2018.08.009.
18. Hsu, P.C., Maity, S., Patel, J., Lupo, P.J., and Nembhard, W.N. (2022). Metabolomics Signatures and Subsequent Maternal Health among Mothers with a Congenital Heart Defect-Affected Pregnancy. Metabolites *12*, 100. https://doi.org/10.3390/metabo12020100.
19. Basu, P., Averitt, D.L., Maier, C., and Basu, A. (2022). The Effects of Nuclear Factor Erythroid 2 (NFE2)-Related Factor 2 (Nrf2) Activation in Preclinical Models of Peripheral Neuropathic Pain. Antioxidants *11*, 430. https://doi.org/10.3390/antiox11020430.
20. Semba, R.D. (2020). Perspective: The Potential Role of Circulating Lysophosphatidylcholine in Neuroprotection against Alzheimer Disease. Adv. Nutr. *11*, 760–772. https://doi.org/10.1093/advances/nmaa024.
21. Law, S.H., Chan, M.L., Marathe, G.K., Parveen, F., Chen, C.H., and Ke, L.Y. (2019). An Updated Review of Lysophosphatidylcholine Metabolism in Human Diseases. Int. J. Mol. Sci. *20*, 1149. https://doi.org/10.3390/ijms20051149.
22. Johnston, E.K., and Abbott, R.D. (2023). Adipose Tissue Paracrine-Autocrine-and Matrix-Dependent Signaling during the Development and Progression of Obesity. Cells *12*, 407. https://doi.org/10.3390/cells12030407.
23. Auger, C., and Kajimura, S. (2023). Adipose Tissue Remodeling in Pathophysiology. Annu. Rev. Pathol. *18*, 71–93. https://doi.org/10.1146/annurev-pathol-042220-023633.
24. Uranbileg, B., Ito, N., Kurano, M., Saigusa, D., Saito, R., Uruno, A., Kano, K., Ikeda, H., Yamada, Y., Sumitani, M., et al. (2019). Alteration of the lysophosphatidic acid and its precursor lysophosphatidylcholine levels in spinal cord stenosis: A study using a rat cauda equina compression model. Sci. Rep. *9*, 16578. https://doi.org/10.1038/s41598-019-52999-5.
25. Liu, M., Xie, Z., Costello, C.A., Zhang, W., Chen, L., Qi, D., Furey, A., Randell, E.W., Rahman, P., and Zhai, G. (2021). Metabolomic analysis coupled with extreme phenotype sampling identified that lysophosphatidylcholines are associated with multisite musculoskeletal pain. Pain *162*, 600–608. https://doi.org/10.1097/j.pain.0000000000002052.
26. Schilling, T., Lehmann, F., Rückert, B., and Eder, C. (2004). Physiological mechanisms of lysophosphatidylcholine-induced de-ramification of murine microglia. J. Physiol. *557*, 105–120. https://doi.org/10.1113/jphysiol.2004.060632.
27. Sheikh, A.M., Nagai, A., Ryu, J.K., McLarnon, J.G., Kim, S.U., and Masuda, J. (2009). Lysophosphatidylcholine induces glial cell activation: role of rho kinase. Glia *57*, 898–907. https://doi.org/10.1002/glia.20815.
28. Kittaka, H., Uchida, K., Fukuta, N., and Tominaga, M. (2017). Lysophosphatidic acid-induced itch is mediated by signalling of LPA(5) receptor, phospholipase D and TRPA1/TRPV1. J. Physiol. *595*, 2681–2698. https://doi.org/10.1113/jp273961.
29. Chen, Y., Wang, Z.L., Yeo, M., Zhang, Q.J., López-Romero, A.E., Ding, H.P., Zhang, X., Zeng, Q., Morales-Lázaro, S.L., Moore, C., et al. (2021). Epithelia-Sensory Neuron Cross Talk Underlies Cholestatic Itch Induced

by Lysophosphatidylcholine. Gastroenterology *161*, 301–317.e16. https://doi.org/10.1053/j.gastro.2021.03.049.

30. Marrone, M.C., Morabito, A., Giustizieri, M., Chiurchiù, V., Leuti, A., Mattioli, M., Marinelli, S., Riganti, L., Lombardi, M., Murana, E., et al. (2017). TRPV1 channels are critical brain inflammation detectors and neuropathic pain biomarkers in mice. Nat. Commun. *8*, 15292. https://doi.org/10.1038/ncomms15292.
31. Dityatev, A., Schachner, M., and Sonderegger, P. (2010). The dual role of the extracellular matrix in synaptic plasticity and homeostasis. Nat. Rev. Neurosci. *11*, 735–746. https://doi.org/10.1038/nrn2898.
32. Alpár, A., Gärtner, U., Härtig, W., and Brückner, G. (2006). Distribution of pyramidal cells associated with perineuronal nets in the neocortex of rat. Brain Res. *1120*, 13–22. https://doi.org/10.1016/j.brainres.2006.08.069.
33. Tajerian, M., Hung, V., Nguyen, H., Lee, G., Joubert, L.M., Malkovskiy, A.V., Zou, B., Xie, S., Huang, T.T., and Clark, J.D. (2018). The hippocampal extracellular matrix regulates pain and memory after injury. Mol. Psychiatr. *23*, 2302–2313. https://doi.org/10.1038/s41380-018-0209-z.
34. Tansley, S., Gu, N., Guzmán, A.U., Cai, W., Wong, C., Lister, K.C., Muñoz-Pino, E., Yousefpour, N., Roome, R.B., Heal, J., et al. (2022). Microglia-mediated degradation of perineuronal nets promotes pain. Science *377*, 80–86. https://doi.org/10.1126/science.abl6773.
35. Mascio, G., Notartomaso, S., Martinello, K., Liberatore, F., Bucci, D., Imbriglio, T., Cannella, M., Antenucci, N., Scarselli, P., Lattanzi, R., et al. (2022). A Progressive Build-up of Perineuronal Nets in the Somatosensory Cortex Is Associated with the Development of Chronic Pain in Mice. J. Neurosci. *42*, 3037–3048. https://doi.org/10.1523/jneurosci.1714-21.2022.
36. Li, X.H., Matsuura, T., Xue, M., Chen, Q.Y., Liu, R.H., Lu, J.S., Shi, W., Fan, K., Zhou, Z., Miao, Z., et al. (2021). Oxytocin in the anterior cingulate cortex attenuates neuropathic pain and emotional anxiety by inhibiting presynaptic long-term potentiation. Cell Rep. *36*, 109411. https://doi.org/10.1016/j.celrep.2021.109411.
37. Cathenaut, L., Leonardon, B., Kuster, R., Inquimbert, P., Schlichter, R., and Hugel, S. (2022). Inhibitory interneurons with differential plasticities at their connections tune excitatory-inhibitory balance in the spinal nociceptive system. Pain *163*, e675–e688. https://doi.org/10.1097/j.pain.0000000000002460.
38. Blom, S.M., Pfister, J.P., Santello, M., Senn, W., and Nevian, T. (2014). Nerve injury-induced neuropathic pain causes disinhibition of the anterior cingulate cortex. J. Neurosci. *34*, 5754–5764. https://doi.org/10.1523/jneurosci.3667-13.2014.
39. Hughes, D.I., Sikander, S., Kinnon, C.M., Boyle, K.A., Watanabe, M., Callister, R.J., and Graham, B.A. (2012). Morphological, neurochemical and electrophysiological features of parvalbumin-expressing cells: a likely source of axo-axonic inputs in the mouse spinal dorsal horn. J. Physiol. *590*, 3927–3951. https://doi.org/10.1113/jphysiol.2012.235655.
40. Rudy, B., Fishell, G., Lee, S., and Hjerling-Leffler, J. (2011). Three groups of interneurons account for nearly 100% of neocortical GABAergic neurons. Dev. Neurobiol. *71*, 45–61. https://doi.org/10.1002/dneu.20853.
41. Li, Q.Y., Duan, Y.W., Zhou, Y.H., Chen, S.X., Li, Y.Y., and Zang, Y. (2022). NLRP3-Mediated Piezo1 Upregulation in ACC Inhibitory Parvalbumin-Expressing Interneurons Is Involved in Pain Processing after Peripheral Nerve Injury. Int. J. Mol. Sci. *23*, 13035. https://doi.org/10.3390/ijms232113035.
42. Decosterd, I., and Woolf, C.J. (2000). Spared nerve injury: an animal model of persistent peripheral neuropathic pain. Pain *87*, 149–158. https://doi.org/10.1016/s0304-3959(00)00276-1.
43. Wang, J., Li, L., Zhang, Z., Zhang, X., Zhu, Y., Zhang, C., and Bi, Y. (2022). Extracellular vesicles mediate the communication of adipose tissue with brain and promote cognitive impairment associated with insulin resistance. Cell Metabol. *34*, 1264–1279.e8. https://doi.org/10.1016/j.cmet.2022.08.004.
44. Chaplan, S.R., Bach, F.W., Pogrel, J.W., Chung, J.M., and Yaksh, T.L. (1994). Quantitative assessment of tactile allodynia in the rat paw. J. Neurosci. Methods *53*, 55–63. https://doi.org/10.1016/0165-0270(94)90144-9.
45. Deng, Z., Li, C., Liu, C., Du, E., and Xu, C. (2018). Catestatin is involved in neuropathic pain mediated by purinergic receptor P2X(4) in the spinal microglia of rats. Brain Res. Bull. *142*, 138–146. https://doi.org/10.1016/j.brainresbull.2018.07.003.
46. Hernandez-Anzaldo, S., Berry, E., Brglez, V., Leung, D., Yun, T.J., Lee, J.S., Filep, J.G., Kassiri, Z., Cheong, C., Lambeau, G., et al. (2015). Identification of a Novel Heart-Liver Axis: Matrix Metalloproteinase-2 Negatively Regulates Cardiac Secreted Phospholipase A2 to Modulate Lipid Metabolism and Inflammation in the Liver. J. Am. Heart Assoc. *4*, e002553. https://doi.org/10.1161/jaha.115.002553.
47. Valle-Dorado, M.G., Hernández-León, A., Nani-Vázquez, A., Ángeles-López, G.E., González-Trujano, M.E., and Ventura-Martínez, R. (2022). Antinociceptive effect of Mansoa alliacea polar extracts involves opioid receptors and nitric oxide in experimental nociception in mice. Biomed. Pharmacother. *152*, 113253. https://doi.org/10.1016/j.biopha.2022.113253.
48. Kong, L., Zhang, Y., Ning, J., Xu, C., Wang, Z., Yang, J., and Yang, L. (2022). CaMKII orchestrates endoplasmic reticulum stress and apoptosis in doxorubicin-induced cardiotoxicity by regulating the IRE1α/XBP1s pathway. J. Cell Mol. Med. *26*, 5303–5314. https://doi.org/10.1111/jcmm.17560.
49. Koyanagi, Y., Oi, Y., and Kobayashi, M. (2021). Fast-spiking Interneurons Contribute to Propofol-induced Facilitation of Firing Synchrony in Pyramidal Neurons of the Rat Insular Cortex. Anesthesiology *134*, 219–233. https://doi.org/10.1097/aln.0000000000003653.

STAR★METHODS

KEY RESOURCES TABLE

REAGENT or RESOURCE	SOURCE	IDENTIFIER
Antibodies		
Wisteria Floribunda Lectin	Vector Laboratories	Cat# FL-1351-2; RRID: AB_2336875
Goat polyclonal Anti-Iba1	Abcam	Cat#ab5076;
Rabbit monoclonal Anti-TRPV1	Abcam	Cat#ab305299;
Rabbit monoclonal Anti-Paralbumin	Cell Signaling Technology	Cat#80561;
Rabbit monoclonal Anti-AIF1/IBA1	Abclonal	Cat#A19776;
Rabbit monoclonal Anti-GAPDH	Abclonal	Cat#A19056; RRID: AB_2862549
Rabbit polyclonal Anti-CaMKII-α	Cell Signaling Technology	Cat# 3357S; RRID: AB_2070308
Rabbit monoclonal Anti-Phospho-CaMKII (Thr286)	Cell Signaling Technology	Cat# 12716; RRID: AB_2713889
Chemicals, peptides, and recombinant proteins		
Varespladib (LY315920)	MedChemExpress	Cat#HY-13402; CAS: 172732-68-2
A-784168	MedChemExpress	Cat# HY-108460; CAS:824982-41-4
KN-93	MedChemExpress	Cat#HY-15465; CAS: 139298-40-1
Chondroitin ABC Lyase	Sigma-Aldrich	Cat#C3667; CAS: 9024-13-9
Tetrodotoxin	CATO Reserch Chemicals Inc.	Cat#CCHM700902; CAS: 4368-28-9
AP-5	Sigma-Aldrich	Cat#A5282; CAS:76326-31-3
CNQX	aladdin	Cat#C131944; CAS:115066-14-3
Critical commercial assays		
LPC (Lysophosphatidyl choline) ELISA Kit	EIK Biotechnology	ELK8145
Deposited data		
Raw data of non-targeted metabolomic analysis	This paper	https://ngdc.cncb.ac.cn/omix: accession no. OMIX007437
Experimental models: Organisms/strains		
Mouse:C57BL/6 male	Beijing Vital River Laboratory Animal Technology Co., Ltd	RRID:MGI:2159769
Software and algorithms		
GraphPad Prism 8	GraphPad Software	https://www.graphpad.com
SPSS 27.0	IBM	https://www.ibm.com

EXPERIMENTAL MODEL AND STUDY PARTICIPANT DETAILS

Animals

Male C57BL/6J mice, aged 8–10 weeks, were purchased from the Beijing Vital River Laboratory Animal Technology Co., Ltd., (Beijing, China). They were housed under standard conditions (room temperature: 22 ± 1°C; relative humidity: 55 ± 5%) and on a 12/12 h light/dark cycle. Animals were randomly assigned to different groups in all experiments. Sample sizes were determined based on similar previous studies in the field. The protocol of all experiments was approved by the Animal Care and Use Committee of Tongji Hospital, and Tongji Medical College approved the current study (no. TJH-20230313).

METHOD DETAILS

Spared nerve injury (SNI)

Mice were deeply anesthetized with isoflurane, placed on an operating table, and subjected to spared nerve injury (SNI) or sham surgeries on the left hind leg. SNI surgery was performed according to the method previously described.[42] Briefly, an incision was made in the skin on the lateral surface of the left thigh, the sciatic

nerve was then exposed after sectioning through the biceps femoris muscle. The sciatic nerve had three terminal branches, the common peroneal and tibial nerves were next tightly ligated with 7–0 silk suture, and 2–3 mm of the nerves distal to the ligation were cut while leaving the sural branch intact. The muscle and skin were closed in separate layers. As for sham surgeries, mice were subjected to exposure of the sciatic nerve and its branches, without any lesions.

Epididymal white adipose tissue transplantation

Fat transplantation was performed as previously described.[4,43] Briefly, epididymal white adipose tissue was isolated from SNI or sham donor mice, and a total of 0.8 g of the donor eWAT was implanted into each recipient mouse. A total of 0.8 g eWAT was cut into approximately 0.1g slices and kept in sterile saline before transplantation. The time of one mouse model of adipose transplantation was about 3 min. The recipient mice were anesthetized with isoflurane, dorsal hair was shaved, the donor fat slices were implanted, and incisions were closed with absorbable sutures. The non-transplanted mice were subjected to exposure of the dorsum with a single cut. During the two weeks after transplantation, recipient mice and sham-operated control mice performed the behavioral test. On day 14 after transplantation, tissues were taken after behavioral tests for follow-up experiments.

Behavioral test

All experiments were conducted between 9 a.m. and 12 a.m. The von Frey test was used to evaluate the mechanical withdrawal threshold. The mice were placed in custom-made Plexiglas cubicles (8 × 8 × 6cm) on a metal mesh floor which allowed full access to the paws. Next, the mice were habituated for at least 1 h before the test. The up-down method of Dixon[44] was used to estimate 50% withdrawal thresholds using calibrated von Frey nylon monofilaments (Stoelting Touch Test). Filaments were applied to the plantar surface of the hind paw for 3 s and responses were recorded. To assess the thermal withdrawal latency, animals were placed in custom-made Plexiglas cubicles (8 × 8 × 6cm) on a glass plate. After the experimental mice became accustomed to the test environment for at least 1 h before testing, thermal radiation (BME-410C Full-automatic Plantar Analgesia Tester; Tianjin, China) was applied to the glass plate in order to heat the plantar of the operated hind paws. The response times until mice moved their paws were recorded. The threshold latencies for each mouse were tested three times and averaged, and each time point was separated by at least 30 min. The longest cut-off latency was set at 30 s to avoid paw injuries.[45]

Non-targeted metabolomic analysis

The eWAT from SNI or sham donor mice were collected. The non-targeted metabolomic analysis was performed by OE Biotech Co. Ltd. Briefly, the 30 mg of total protein from individual samples was prepared. ACQUITY UPLC I-Class system (Waters Corporation，Milford, USA) coupled with VION IMS QTOF Mass spectrometer (Waters Corporation，Milford, USA) was used to analyze the metabolic profiling in both ESI positive and ESI negative ion modes. An ACQUITY UPLC BEH C18 column (1.7μm, 2.1 × 100 mm) were employed in both positive and negative modes. The original LC-MS data were processed using software Progenesis QI V2.3 (Nonlinear, Dynamics, Newcastle, UK) for baseline filtering, peak identification, integral, retention time correction, peak alignment, and normalization. A two-tailed Student's T-test was further used to verify whether the different metabolites between groups were significant. Differential metabolites were selected with VIP values greater than 1.0 and p-values less than 0.05.

Immunohistochemistry

Mice were deeply anesthetized with sodium pentobarbital and perfused intracardially with PBS followed by 0.1M phosphate buffer (4% paraformaldehyde, PFA, pH 7.4). For brain sections, mouse brains were fixed in 4% PFA for 24 h, followed by soaking in 15% and 30% sucrose solution for dehydration. The brains were then cut into coronal sections at 30 μm thickness by a CryoStar NX50 (Thermo Scientific, Rockford, IL, USA). For immunofluorescence staining, tissue sections were blocked in 10% normal donkey/goat serum (NGS/NDS) with 0.3% Triton X-100 in PBS for 1 h before incubation with primary antibodies at 4°C overnight. For perineuronal nets staining, Wisteria Floribunda Lectin ([1:400], Vector Laboratories FL-1351-2) was utilized. We used Iba-1 ([1:100], ABclonal A19776), Wisteria Floribunda Lectin ([1:400], Vector Laboratories FL-1351-2) for microglial engulfment staining and for double-labeled immunofluorescence Iba-1 ([1:1000], Abcam ab5076), TRPV1([1:500], Abcam ab305299), Paralbumin ([1:1000], CST 80561). Then, after 3 washes, the sections were incubated with appropriate fluorescent secondary antibodies for 2 h at room temperature. Secondary antibodies 1:400 Donkey anti-goat Alexa Fluor 647 [Jackson, AB2340437] 1：400 Goat anti-rabbit Alexa Fluor CY3[Jackson, AB2338006], 1：400 Donkey anti-rabbit Alexa Fluor CY3[Jackson, AB2307443]，Donkey anti-rabbit Alexa Fluor 488 [Jackson, AB2313584], 1：400 Donkey anti-mouse Alexa Fluor CY3[Jackson, AB2340813], were applied. Tissue was stained with DAPI [Beyotime, C1005] before image capture using a Leica TCS SP8 confocal microscope or Olympus VS120 Virtual Slide Microscope.

Elisa test

Brain tissue and serum were collected from experimental mice and kept at −80°C. According to the manufacturer's instructions, a commercial ELISA kit (EIK Biotechnology) was employed to quantitatively estimate the levels of lysophosphatidylcholine.

Western blot analysis

After mice completed the behavioral pain tests, the anterior cingulate cortex was removed. Protein was extracted from tissues using RIPA lysis buffer (Thermo Scientific, Rockford, IL, USA) supplemented with protease and phosphatase inhibitors, and the protein concentration was quantified using a BCA protein assay kit (Thermo Scientific). Then, 30 μg of protein lysates was loaded into SDS/PAGE gels, followed by the transfer to polyvinylidene difluoride (PVDF) membranes (Millipore). The membranes were probed with various primary antibodies after blocking with 5% nonfat milk for 1h. The following primary antibodies were used: GAPDH ([1:10000], ABclonal A19056) Phospho-CaMKII (Thr286) (D21E4) ([1:1000], CST 12716T), CaMKII-α Antibody ([1:1000],

CST3357S), TRPV1([1:500], Abcam ab305299). The membrane was incubated overnight at 4°C with primary antibodies. After the blots were washed three times, the membranes were incubated with horseradish peroxidase (HRP)-conjugated secondary antibodies and visualized using an ECL Western blotting Detection Kit (Thermo Scientific). For quantification, the densities of protein bands were digitized using the ChemiDoc MP Imaging System. Protein levels were analyzed ImageJ analysis software.

In vivo pharmacological studies

To study the effect of LPC in hyperalgesia, we utilized the phospholipase A2 inhibitor varespladib (MedChemExpress, Monmouth junction, NJ, USA, HY-13402). Mice were gavaged with the varespladib (10 mg/kg per day) from day 9 to day 12 after transplantion.[46] The varespladib powder was prepared according to the manufacturer's instructions. We used the following cosolvents in 10% DMSO+40% PEG300 + 5% Tween-80 + 45% Saline to dilute before the experiment. The $Trans^{Sham}$ group were given the same diluent without pharmaceutical. To verify the effect of TRPV1, we administered its inhibitor A-784168 (1 mg/kg/d) (MedChemExpress, Monmouth junction, NJ, USA HY-108460) through intraperitoneal injection for four consecutive days from day 9 to day 12 after transplantation.[47] The CamkII inhibitor KN-93 (MedChemExpress, Monmouth junction, NJ, USA, HY-15465) was then given through intraperitoneal injection (3 mg/kg/d) for four consecutive days from day 9 to day 12 after transplantation.[48] The dose regimen was followed based on previous reports.

ACC injection

We administered protease-free chABC (Sigma-Aldrich) to degrade the PNNs in the ACC. ChABC was dissolved to 50 U/ml in PBS containing 0.1% BSA and filtered through a 0.2 mm filter.[35] The mice were anesthetized using isoflurane, and a small hole was drilled in the skull (AP, 0.38 mm; ML, 0.5 mm; DV, −1.85 mm; stereotactic coordinates corresponding to the mouse brain atlas). Then, the mice were injected with chABC (0.5ul each at 0.1ul/min) using a 1μL Hamilton syringe. Control mice were infused with vehicle (PBS containing 0.1% BSA).

Electrophysiology recording

The whole-cell recordings were performed *in vitro* from the ACC region neurons, aimed to examine the changes in inhibitory interneurons. We immersed the brain into the cold oxygenated cutting solution after anesthesia and then sliced it into 300 μm sections using the vibratome (VT1200S; Leica, Germany). The individual slice was incubated for at least 1 h at 30°C in oxygenated artificial cerebrospinal fluid (ACSF), then placed in the submersion-recording chamber, and perfused with ACSF (2 mL/min). The ACSF was made utilizing (in mM): 125.0 NaCl, 1.2 NaH_2PO_4, 26.0 $NaHCO_3$, 5.0 KCl, 2.6 $CaCl_2$, 1.3 $MgCl_2$, and 10.0 glucose. Each slice only recorded one neuron. Data acquisition and analysis of the electrical signals were performed with the Axonpatch 700B Amplifier (Molecular Devices, USA), the Digidata 1500B Digital Converter (Molecular Devices, USA), and the pClamp 10 software (Molecular Devices, USA). Inhibitory interneurons in the ACC region were identified by accommodating responses to a sustained depolarizing intracellular current stimulation, fast-spiking neurons (firing rate >10 Hz) with shorter duration waveforms believed to correspond to the inhibitory interneurons.[49] The WPI recording pipettes (4–7 MΩ, USA) were filled with the pipette solution containing (in mM), 100 KCl, 40 HEPES, 0.2 EGTA, 5 $MgCl_2$, 2.0 Mg-ATP, 0.3 Na_3-GTP, 10 phosphocreatine (pH 7.30 and 300 mOsm/kg). The miniature inhibitory postsynaptic currents (mIPSCs) were pharmacologically isolated using CNQX (10μM), AP-5 (100μM), and TTX (1 μM), and recorded at − 70 mV. For analysis, we recorded a fixed 5-min length of traces.

QUANTIFICATION AND STATISTICAL ANALYSIS

All results were expressed as mean ± standard error of the mean (SEM). Statistical differences between groups were analyzed by either one-way ANOVA followed by Tukey's post-hoc comparison, two-way ANOVA followed by Sidak's post-hoc comparison, the Mann-Whitney U test or unpaired Student's t test, using SPSS 27.0 software (IBM) and Statistical GraphPad Prism 8 software (La Jolla, USA). Sample size (n) is listed in each figure legend. Differences were considered statistically significant when $p < 0.05$. All the detailed statistical information relative to the figures are in the Table S1.